Control of a 1051 nm fiber laser for the Doppler cooling of Be^+ ions

A.Franck[a]

a. Mines Paris PSL + antonin.franck@etu.minesparis.psl.eu

Mots clés : Laser cooling ; Frequency comb ; Fiber laser ; Laser control ; REFIMEVE ; Nonlinear optics

Abstract :
This paper focuses on the control of a 1051 nm fiber laser, which is useful for the laser cooling of Be^+ ions, in the frame of the H_2^+ high resolution spectroscopy project developped at Kastler Brossel laboratory (LKB). It is locked on a frequency comb, which is locked on the REFIMEVE ultrastable signal disseminated by SYRTE laboratory. We present why we need this precise laser source and all the experimental set up. The results show that the frequency noise contributes on the wings but not on the linewidth of the laser. A very precise 1051 nm laser source is obtained.

1 Introduction

This paper arises from the project of achieving high-resolution Doppler-free two-photon vibrational spectroscopy on the H_2^+ ion. The purpose of this experiment is to measure $\mu_{pe} = m_p/m_e$, the proton to electron mass ratio. At present, the uncertainty on μ_{pe} given by the CODATA organisation is $6,0.10^{-11}$ [1], and this ratio is obtained by precise measurements of m_e [2] and m_p [3]. The idea of performing vibrational spectroscopy on a simple molecular ion (HD^+) in order to determine μ_{pe} dates back to 1976 [4]. It can be an efficient technique, because the most precise measurements are achieved with measurements of narrow lines frequency. In 2001, it has been shown [5] that we could perform the spectroscopy of H_2^+ for a simpler determination of μ_{pe} (with HD^+, two measurements were necessary against one with H_2^+). Actually, these experiments can be complementary in order to determine several fundamental constants relevant for atomic physics [6] : R_∞ : the Rydberg constant, μ_{pe}, $\mu_{dp} = m_d/m_p$, r_d : the deuteron radius, r_p : the proton radius. Currently, the spectroscopy of HD^+ has already been performed, with one-photon vibrational transitions, but it is not the case for H_2^+, which is slightly different because it does not have a electric dipole moment and thus, one-photon vibrational transitions are forbidden. The probability of a two-photon vibrational transition is generally several orders of magnitude smaller and a lot of power is needed. This explains partly why this has never been made.

To realize the high-resolution spectroscopy, it is needed to cool the H_2^+ ions in order to reduce the second order Doppler effect (otherwise, the relative effect on the transition frequency is about $5,0.10^{-10}$ [7]). The technique used is sympathetic cooling [8, 9] because we cannot cool H_2^+ with laser sources. It depends on the Coulomb interaction between H_2^+ and a laser-cooled species : in our experiment, Be^+ is chosen because the closer the masses of the two species, the more efficient the cooling. The idea is to trap the two types of ions together in a linear Paul trap [10], and to cool the Be^+ ions with a laser. In this trap, there are good access for imaging system and laser sources. This laser cooling was proposed in 1975 [8, 11] but we had to wait until 1978 to put this idea in place [8] because tunable laser sources were necessary, and they did not exist at the time. In order to cool the Be^+ ions, we need a 313 nm laser source. Nowadays, there are not semiconductor that emit at 313 nm, so we need a more elaborated technique. The 313 nm laser is obtained by the frequency sum of two fiber lasers at 1051 nm and 1550 nm followed by frequency doubling of the resulting 626 nm light [12]. Indeed, $2\left(\frac{c}{\lambda_1}+\frac{c}{\lambda_2}\right)=\frac{c}{\lambda_3}$ with $\lambda_1 = 1051$ nm, $\lambda_2 = 1550$ nm, $\lambda_3 = 313$ nm. In this paper, we will focus especially on the control of the 1051 nm laser fiber by a frequency comb which is locked on REFIMEVE, an ultra-stable signal from the SYRTE. We need the frequency of this laser to be very precise (below 100 kHz accuracy) in order to realize the transition that cools the ions.

Firstly, we will bring the theory of Doppler cooling up, as well as the way to generate the 313 nm laser. Then, we will focus on the 1051 nm laser frequency control. We will explain the experimental set-up and then show the results, especially the reduction of the frequency noise.

2 Trapped ions cooling

2.1 Doppler cooling of an atom

In order to cool trapped ions, we can use Doppler cooling. It relies on the mean force applied on an atom by a laser. Let us suppose that the atom is a two-level E_0 and E_1 dipole system, moving at speed $\mathbf{v}$. The excited level E_1 can transit to the fundamental level E_0 by spontaneous emission. The difference of energy is noted $\hbar\omega_{at}$, and the natural linewidth of the transition is Γ. The laser source emits traveling plane waves at the frequency $\omega/2\pi$. We suppose also that the laser detuning $\delta = \omega - \omega_{at}$ is of the order of Γ. In that case, the absorption of a photon permits the atom to reach its excited level. At that time, its momentum is given by :

$$\mathbf{p} = m\mathbf{v} - \hbar\mathbf{k} \tag{2.1}$$

Then, there are two possibilities, either the atom go back to its fundamental level by spontaneous emission (step 3 in Figure 1) and it changes its momentum into $m\mathbf{v} - \hbar\mathbf{k} - \hbar\mathbf{k}_{sp}$, or by stimulated emission (step 2 in Figure 1) and its momentum's variation is canceled . This process is repeated many times during a period T. During the spontaneous emission, there is no preferential direction, so we have :

$$\langle \hbar\mathbf{k}_{sp} \rangle_T = 0 \Rightarrow \langle \mathbf{p} \rangle_T = m\mathbf{v} - n\hbar\mathbf{k} \tag{2.2}$$

with n the number of cycles where there is spontaneous emission. Therefore, it seems possible to slow an atom with lasers.
Actually, the atom is subject to a mean force, given by [7] :

$$\mathbf{F} = \frac{\Gamma\hbar\mathbf{k}}{2}\frac{s}{1+s} \tag{2.3}$$

with[1] $s = \frac{\Omega_R^2/2}{(\delta - \mathbf{k}\cdot\mathbf{v})^2 + \Gamma^2/4}$ and where $\Omega_R = \Gamma\sqrt{\frac{I}{2I_{sat}}}$. This overall process is shown in Figure 1.

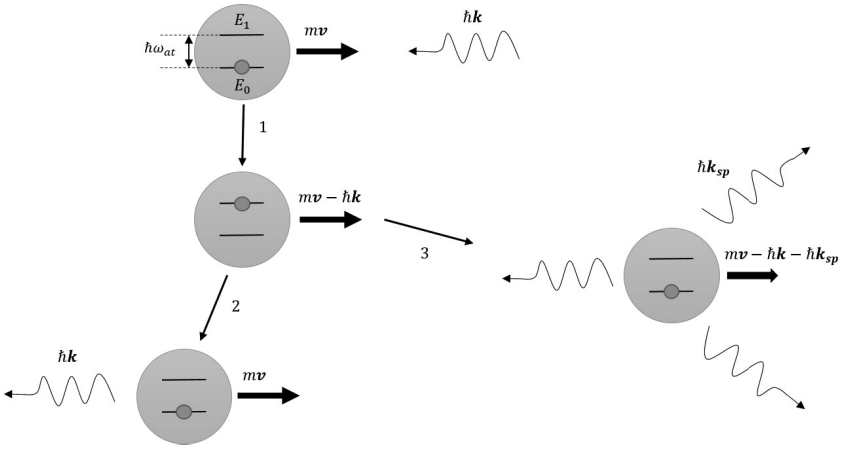

Figure 1: Schema of Doppler cooling

2.2 Doppler cooling of a trapped ion

At first glance, one cannot use (2.3) on a trapped ion. However, under certain conditions [13], the effective potential that trap the ion is harmonic with pulsations $\omega_{x,y,z}$, and if $\Gamma \gg \omega_{x,y,z}$, (2.3) is a good approximation of the interaction between light and matter.
In the rest of this part, we will focus of the ion's motion in 1D. Thanks to Newton's second law, the position z of a trapped ion, illuminated by a laser on the $\mathbf{z}$ direction, is given by :

$$\ddot{z} - \frac{\hbar k\Gamma}{2}\frac{\Omega_r^2/2}{(\delta - k\dot{z})^2 + \Gamma^2/4 + \Omega_r^2/2} + \omega_z^2 z = 0 \tag{2.4}$$

[1] The term $\mathbf{k}\cdot\mathbf{v}$ comes from the Doppler effect.

We are interested in the transition between $^2S_{1/2}(F=2)$ and $^2P_{3/2}$, whose natural linewidth is $\Gamma = 19,4$ MHz. As we said in the introduction, we use a 313 nm laser source to cool the Be^+ ions, so $k \simeq 2,0.10^7$ m^{-1}.

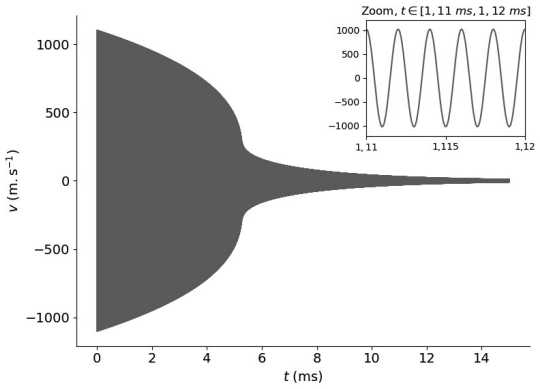

Figure 2: Evolution of a Be^+ ion's speed during Doppler cooling, with $\delta = -50\Gamma$, $I/I_{sat} = 10$, $\omega_z/2\pi =$ 500 kHz, $z_0 = 0$ and $\dot{z}_0 = 1100$ m/s

The equation (2.4) is numerically solved with *Python* in Figure 2, using `odeint` function from the `scipy.integrate` library. The figure shows that the velocity oscillates with time with a decreasing amplitude. The inset zooms on few oscillation periods. We can see that the cooling (amplitude's variation) is slow until $t \simeq 5$ ms, where the speed falls and then the slow cooling pick up again. In practice, we can use a great detuning to slow the fast ions and then reduce it to slow efficiently the slow ions[2].
In theory, the ions' speed should tend toward 0, so their temperature should reach $T = 0$ K. But, in fact, the force applied on the ions fluctuates randomly because of the spontaneous emission of photons. This effect warms them. The minimal temperature we can achieve comes from the equilibrium between Doppler cooling and this warming. We can show [13] that this minimal temperature is obtained with a detuning of $\delta = -\dfrac{\Gamma}{2}$ and a small intensity $I \to 0$ and is :

$$T_{min} = \frac{\hbar\Gamma}{2k_B} = 0,47 \text{ mK} \tag{2.5}$$

The following section describes how to obtain the laser at 313 nm, needed for the Doppler cooling.

2.3 Frequency sum and doubling

2.3.1 Reminder of linear optics

In linear optics, there is a linear response of the polarization $\mathbf{P}_\text{L}$ to the excitation by an electric field $\mathbf{E}$. One can write it as :

$$\mathbf{P}_\text{L} = \varepsilon_0 \underline{\underline{\chi}} \mathbf{E} \tag{2.6}$$

This formula is true when $||\mathbf{E}||$ is small. The second-order tensor $\underline{\underline{\chi}}$ is called the susceptibility of the medium. It depends on the structure of the medium, and it is linked with the index by :

$$n = 1 + \underline{\underline{\chi}} \tag{2.7}$$

2.3.2 Principles of nonlinear optics

When $||\mathbf{E}||$ becomes large, the polarization cannot respond linearly anymore. In this case, the polarization can be expanded in power of the field as :

$$\mathbf{P} = \varepsilon_0 \underline{\underline{\chi}}^{(1)} \mathbf{E} + \varepsilon_0 \underline{\underline{\chi}}^{(2)} \mathbf{EE} + \varepsilon_0 \underline{\underline{\underline{\chi}}}^{(3)} \mathbf{EEE} + ... = \mathbf{P}_\text{L} + \mathbf{P}_\text{NL} \tag{2.8}$$

where $\chi^{(n)}$ is a $(n+1)$-order tensor. In practice, only the terms with $n \leq 3$ are not negligible.

[2] We can also do that with two lasers (one with a great $|\delta|$ and the other with a small $|\delta|$).

In this section, we will focus on the effects of $\chi^{(2)}$. Let us suppose that we have a wave described by $\tilde{\mathbf{E}}(\mathbf{r},t) = \sum_n \mathbf{E}(\omega_n)e^{i\omega_n t}$, with $\mathbf{E}(\omega_n) = \mathbf{A}(\omega_n)e^{i\mathbf{k}_n\cdot\mathbf{r}}$, and $\mathbf{E}(-\omega_n) = \mathbf{E}(\omega_n)^*$. Let $\mathbf{e}_i$ denote the canonical basis of $\mathbb{R}^3$. If we look only at the second-order term, it appears[3] that [14] :

$$P_{\mathrm{NL},i}(\omega = \omega_n + \omega_m) = \mathbf{P}_{\mathrm{NL}} \cdot \mathbf{e}_i = \varepsilon_0 \sum_{k,l} \sum_{n,m} \chi^{(2)}_{ijk}(\omega = \omega_n + \omega_m, \omega_n, \omega_m) E_j(\omega_n) E_k(\omega_m) \tag{2.9}$$

The summation is such that $n,\ m$ vary, but ω is fixed. The product $E_j(\omega_n)E_k(\omega_m)$ leads to a contribution to $\mathbf{P}_{\mathrm{NL}}$ which oscillates at the frequency $\omega_n + \omega_m$. If the field is resulting of two harmonic waves of frequencies ω_1 and ω_2, it looks possible to obtain a wave oscillating at the frequency $\omega_3 = \omega_1 + \omega_2$. But, there is another condition that needs to be respected, in order to obtain a powerful wave : the phase velocities of the two waves (the intput wave and the "generated wave" oscillating at ω_3) must match [15]. If not, they will interfere destructively. This is called phase matching. As a reminder, the phase velocity v_φ is defined as :

$$v_\varphi = \frac{\omega}{k} = \frac{c}{n(\omega)} \tag{2.10}$$

with $n(\omega)$ the index of refraction of the medium at the pulsation ω.
To simplify, we will handle the case of the frequency doubling, that is to say that :

$$\omega_1 = \omega_2 \overset{\text{def}}{=} \omega \tag{2.11}$$

The phase matching condition implies that :

$$\mathbf{k}_3(2\omega) = \mathbf{k}_1(\omega) + \mathbf{k}_2(\omega) \tag{2.12}$$

That is to say that the momentum must be conserved. If all the $\mathbf{k}_i$ are collinear, the condition (2.12) simplifies into :

$$2\omega \times n(2\omega) = 2\omega \times n(\omega) \Leftrightarrow n(2\omega) = n(\omega) \tag{2.13}$$

It means that the wave at a frequency 2ω will be powerful if the condition (2.13) is verified. In general, it is not the case, because of dispersion in the medium. Luckily, we can use birefringent crystals. In such a medium, there are generally two index n_o and n_e (index of the ordinary and extraordinary beams respectively), that depends on the direction of propagation and the polarization of the wave. The condition (2.13) can be satisfied if :

$$n_e(2\omega) = n_o(\omega) \tag{2.14}$$

It has been shown, that with a carefully chosen angle between the incident beam and the optical axis, the condition (2.14) is satisfied and a powerful wave at a pulsation 2ω is generated. With other non linear crystals, one can also generate a powerful wave, whose frequency is the sum of the two interacting waves' frequencies.
To conclude this section, the need of a precise laser source at 313 nm for Doppler cooling required to understand a little of nonlinear optics. With two crystals (a periodically poled lithium niobate (PPLN) and a beta barium borate (BBO)), we can sum two lasers at 1051 nm and 1550 nm to get 626 nm and and then double the frequency in order to obtain a source at 313 nm. The following section focuses on the control of the 1051 nm fiber laser.

3 1051 nm fiber laser control

In this experiment, we observed the beat-note between the 1051 nm extension of a comb described in section 3.1.2 and a fiber laser at 1051 nm. The idea was to control the fiber laser frequency used for ion cooling with the frequency comb and no more with a wavemeter, which is less precise. As a reminder, the beat-note is obtained when mixing two laser sources and measuring the mixed signal with a photodiode. If the two signals are $E_l = E_l^0 e^{i(\omega_l t - \mathbf{k}\cdot\mathbf{r} + \varphi_l)}$ with $l \in \{1,2\}$ and $E_l^0 \in \mathbb{R}$, then the intensity I is proportional to $|E|^2$, and in $\mathbf{r} = \mathbf{0}$:

$$|E|^2 = (E_1^0)^2 + (E_2^0)^2 + E_1^0 E_2^0 \cos\left((\underbrace{\omega_1 - \omega_2}_{\mathrm{beat-note}})t + \varphi_1 - \varphi_2\right) \tag{3.1}$$

If we formulate the hypothesis that the frequency comb's spectrum does not fluctuate (since it is locked on REFIMEVE, it is almost true), the control of the beat-note is equivalent to the control of the laser frequency.

[3] The summation is on both the positive and negative frequencies.

3.1 Protocol

3.1.1 Equipment

In this experiment, we used mainly a fiber laser at 1051 nm, a frequency comb, a reflective grating, a fiber coupler, a photodiode, a spectrum analyser, a PFD (Phase Frequency Detector) circuit and a P-I (Proportional Integrator) controller.

3.1.2 Frequency comb

The LKB have a frequency comb, which is a laser source that emits a regularly spaced succession of pulses. In the frequency domain, the spectrum is a comb with a tooth spacing f_{rep}. It can emit at a lot of frequencies because its active laser medium is a glass and not a crystal, so it is spatially inhomogeneous. The tooth spacing is a constant because of very nonlinear effects that will not be described in this paper. A N teeth frequency comb is equivalent to N continuous lasers, with frequencies equidistant of f_{rep}, that are equal to $pf_{rep} + f_0$, with $p \in [\![-N/2, N/2]\!]$ (f_0 is an offset, but our comb is such that $f_0 = 0$ Hz). $f_c = \omega_c/2\pi$ is the central frequency of the comb. Its electric field is given by :

$$\mathbf{E}(\mathbf{r}, t) = \mathbf{e} \sum_{p=-\frac{N}{2}}^{\frac{N}{2}} E_p e^{i((\omega_c + p\omega_{rep})t - \mathbf{k_p}\cdot\mathbf{r} - \phi_p)} \tag{3.2}$$

with $\omega_{rep} = 2\pi f_{rep}$, $\mathbf{k}_p$ the wave vector of the tooth p, $\mathbf{r}$ the position in space, E_p and ϕ_p the amplitude and phase of each mode. In the ideal case : $\forall p \in [\![-N/2, N/2]\!],\ E_p = E_0\ ;\ \phi_p = 0$, one can obtain :

$$\mathbf{E}(\mathbf{r} = \mathbf{0}, t) = \mathbf{e} E_0 e^{i\omega_0 t} \frac{\sin\left((N+1)\omega_{rep} t/2\right)}{\sin(\omega_{rep} t/2)} \tag{3.3}$$

Then,

$$I \propto ||\mathbf{E}||^2 \propto \left(\frac{\sin\left((N+1)\omega_{rep} t/2\right)}{\sin(\omega_{rep} t/2)}\right)^2 \tag{3.4}$$

The intensity has the same shape as in the case of a grating (if we replace the angle θ by the time t) : there are short pulses spaced of $T_{rep} = 1/f_{rep}$.

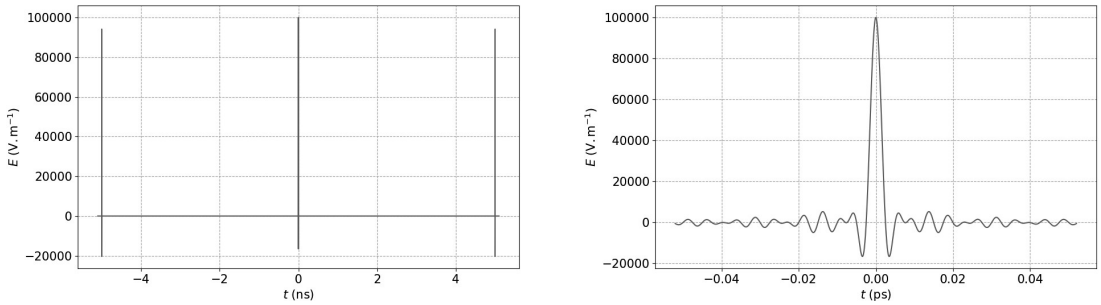

Figure 3: Intensity of the comb in the ideal case. Right : Zoom on the central peak : the pulse width is 100 fs

In our frequency comb, ω_c is such that $\lambda_c \simeq 1,56$ µm. We can then lock it on the REFIMEVE signal, whose frequency is $f_{\text{REFIMEVE}} = 194\ 400\ 008\ 500\ 000 \pm 2$ Hz, being $\lambda_{\text{REFIMEVE}} \simeq 1,542$ µm.

3.1.3 Frequency comb's extension

Fortunately there is an extension of the frequency comb at 1051 nm. That is to say that there is a source with the same features as in section 3.1.2 but centered at 1051 nm, which is the wavelength of the laser we want to control. Its spectrum is given in Figure 4.
Firstly, we brought this extension of the frequency comb with an optical fiber. We put an optical filter (in order to keep only the comb teeth around 1051 nm) and tested the power in free space of the laser in function of the pump percentage. The extension is obtained by amplifying the comb and then injecting it into a very nonlinear fiber. The pump percentage is the level of this amplification. It is the only available parameter to control the comb extension.

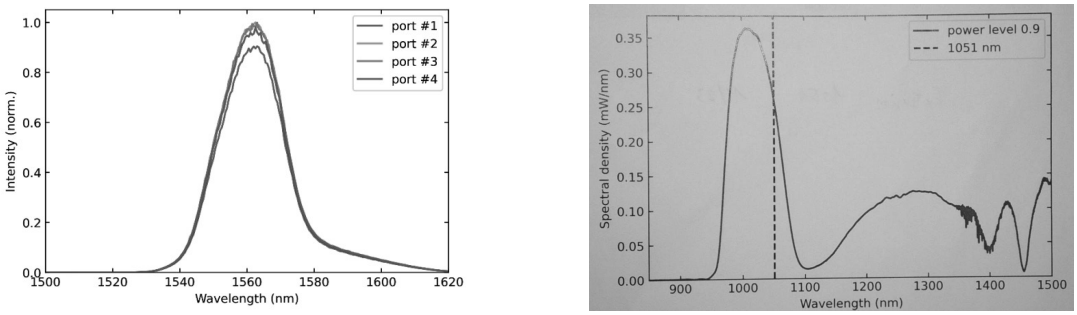

Figure 4: Spectra of the comb (left) and its extension (right) at 1051 nm from comb datasheet. The pump percentage of the extension is 90%.

We have commissioned the comb extension observing that we got the maximum of power with 90% of pumping as indicated on the laser test report. The beat-note is between the fiber laser and a single spectral line of the comb. We estimated that approximately 14000 lines pass through the filter. Indeed, the optical filter has a full width at half maximum (FWHM) of 10 nm : $\Delta\lambda = 10$ nm. Yet, $\nu = c/\lambda$, so $\Delta\nu = c/\lambda^2 \times \Delta\lambda$. The substitution in the formula gives $\Delta\nu \simeq 2,716$ THz. Since the comb tooth spacing is 200 MHz, there are 5 teeth in 1 GHz and then, 13 579 teeth in 2,716 THz. After the filter, the power of the comb is around 1,7 mW so the power of a tooth is around $1,7.10^{-3}/13579 \simeq 0.125$ µW which is sufficient to observe the beat-note.

3.1.4 Reflective grating

We used a grating to reduce the number of lines that pass through the system, in order to cut the wrong lines, whose energy would just saturate the photodiode. We needed a grating for which there is at least an order (other than 0, which is the classic reflection). The possibilities are given by the reflective grating equation :

$$\sin(i) + \sin(\theta) = \frac{p\lambda}{a} \tag{3.5}$$

With a groove density of 1200 g/mm, and an angle of incidence of 45°, the angle of the first (and unique) order beam is approximately 33°. But in this case, we can see on Figure 5 that the angular spacing is almost at the minimum. We should work in lower incidence, but there will be a compromise between angular spacing and intensity. With the grating that we have (a blazed grating with a blaze angle of 26°), the signal-to-noise ratio of the beat-note appears to be better at 45°.

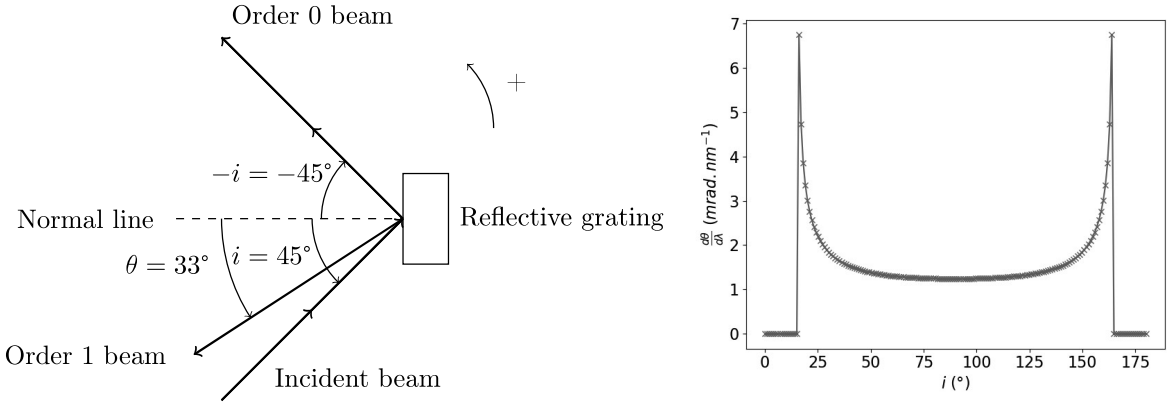

Figure 5: Left : Schema of a reflective grating, with $n = 1200$ grooves/mm and $\lambda = 1051$ nm with oriented angles. Right : angular spacing in function of incident angle

After diffraction on the grating, we needed to put the beam back in an optical fiber, in order to mix the two signals (from the comb and from the fiber laser). To do that, we put a laser at the output and we tried to stack the two beams. There were four degrees of freedom : two rotations around a vertical axis and two other rotations around a horizontal axis (two screws for the mirror and two for the grating). We

used a technique called "clic-clac", which consists in repeatedly moving a screw and then optimize with the other. There was two "clic-clac" to do : one for the vertical screws and another one for the horizontal screws.

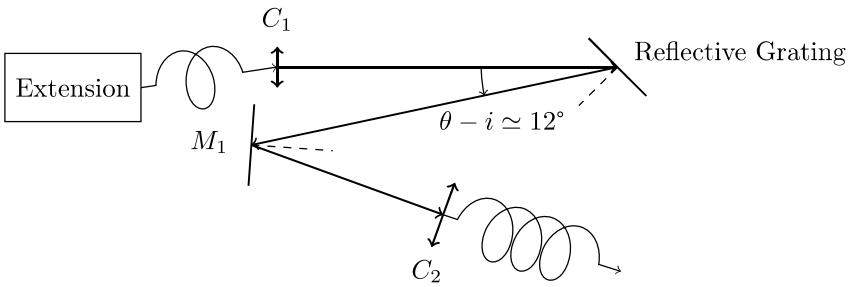

Figure 6: Schema of the "clic-clac" set-up. M_1 : PF10-03-M01-10. C_1 : F260 APC-B

3.1.5 Mixing

We mixed the two lasers (fiber laser and extension of the frequency comb) with a 75/25 coupler (it means that 75% of the energy of the first source and 25% of the second source pass through the system). We kept 75% of the energy of the comb because it is much less powerful than the fiber laser (1, 7 mW after the filter against 10 mW)

3.1.6 Spectrum analyzis

The frequencies that are there are too high ($\lambda = 1051$ nm is equivalent to $\nu = 285$ THz) for direct electronic instruments, so we used a photodiode in order to work at acceptable frequency. We could use also an attenuator in order not to saturate the photodiode. We plugged the beat-note signal in a spectrum analyzer and observed the beat-note and the comb tooth spacing f_{rep}.

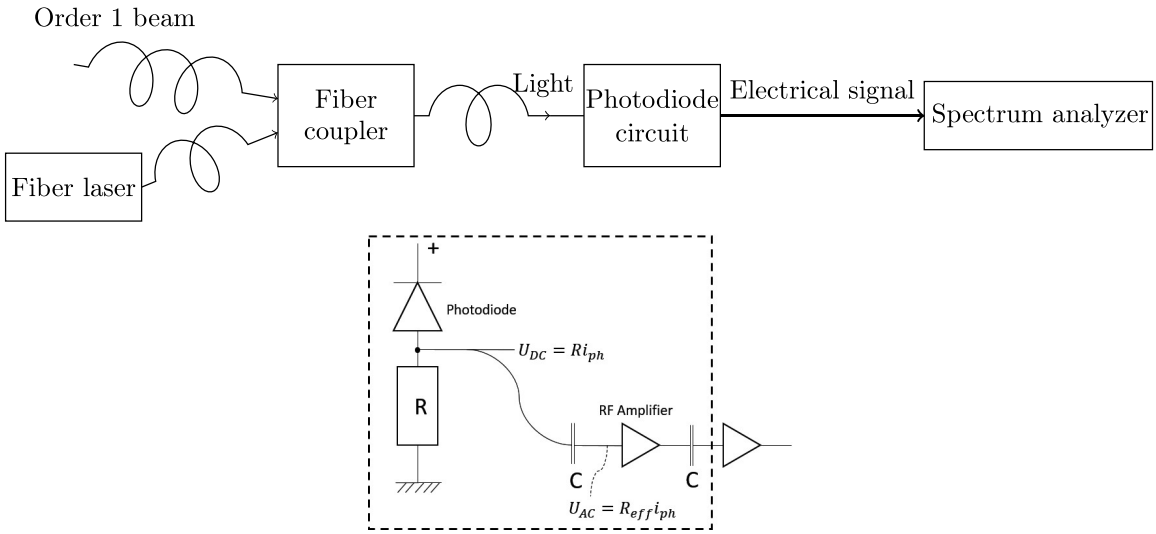

Figure 7: Top : Schema of mixing and analyzis set-up. Fiber coupler : Koheron FOSPL12-7525. Spectrum Analyser : Rigol DSA 815-TG. Bottom : Zoom on the photodiode circuit

3.2 Results and improvements

We saw several beat-notes, there is one between each comb tooth that reentered in the fiber and the fiber laser.

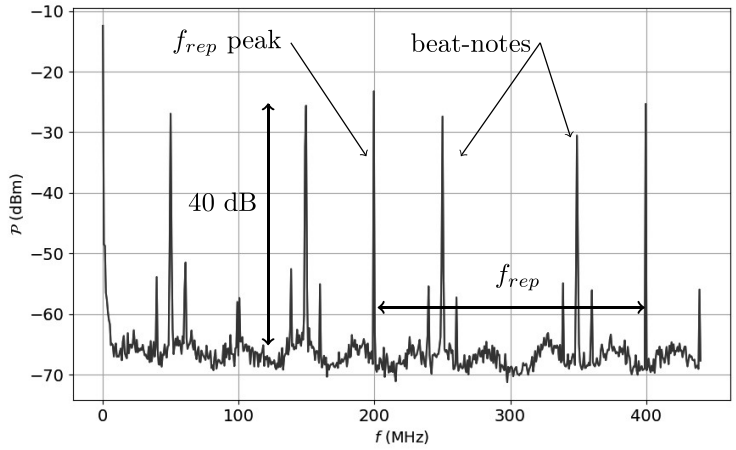

Figure 8: Beat-note signal before the band-pass filter. Bandwidth : 100 kHz. Comb's power : 2 μW, fiber laser's power : 600 μW.

After these first results, we improved the experiment. We needed to control the polarization, because the beatnote is proportional to the polarization dot product $\mathbf{P}_1 \cdot \mathbf{P}_2$, so we added a polarization controller between the fiber laser and the fiber coupler.
We obtained a better signal-to-noise ratio (SNR)[4] :

$$\mathrm{SNR}_{dB} = \mathcal{P}_{\mathrm{signal,dBm}} - \mathcal{P}_{\mathrm{noise,dBm}} \simeq (-28) - (-68) = 40 \text{ dB} \tag{3.6}$$

3.3 Control

To control the fiber laser frequency, we needed to extract the beat-note between this laser and a unique comb tooth, so we used a band-pass filter with a very thin bandwidth. The phase/frequency noise of the laser is included in the beat-note signal, as shown in equation (3.1).
In order to control a laser frequency, one has to generate an error signal depending on the distance with the setpoint (the desired value). This signal goes then through a feedback loop. To make an error signal, we used a phase frequency detector (PFD). We used it in a phase-locked loop (PLL).

3.3.1 Error signal

We want to create a signal which is proportional to the difference of phase of two signals $s_1(t) = \sin(\omega_1 t + \varphi_1)$ and $s_2(t) = \sin(\omega_2 t + \varphi_2)$
To simplify, the idea behind the PFD is the "exclusive or" (XOR). There is a prescaler that reshapes the sinusoidal signals into square signals, and then the two signals pass into a XOR gate and a low-pass filter that keeps only the mean of the signal. When the phases are close, the filter returns 0 because A XOR A = 0, and when the phases are very different (modulo 2π), the filter returns 1 because A XOR NOT(A) = 0. The actual behaviour of the PFD is given in Figure 9.
In practice, it is more complicated and there are 3 possibilities. If $\omega_1 > \omega_2$, the output is positive, and if $\omega_2 > \omega_1$, the output is negative. The interesting situation is when $\omega_2 = \omega_1$, because in this case, the output takes the shape of triangles.
In our situation, the two signals are the beat-note and a signal generated by a frequency synthesizer which is a reference. We did not use its internal quartz, but an external precise reference at 10 MHz which comes from the SYRTE laboratory.

3.3.2 PLL

To complete our control, we used a proportional-integral controller, and we adjusted it in order to have the thinest and greatest peak of beat-note signal (we were looking for the best noise-to-signal ratio).

[4]The bandwidth is 100 kHz.
[5]50% of the energy goes in the spectrum analyzer and 50% in the control circuit.

Annotation en haut à gauche

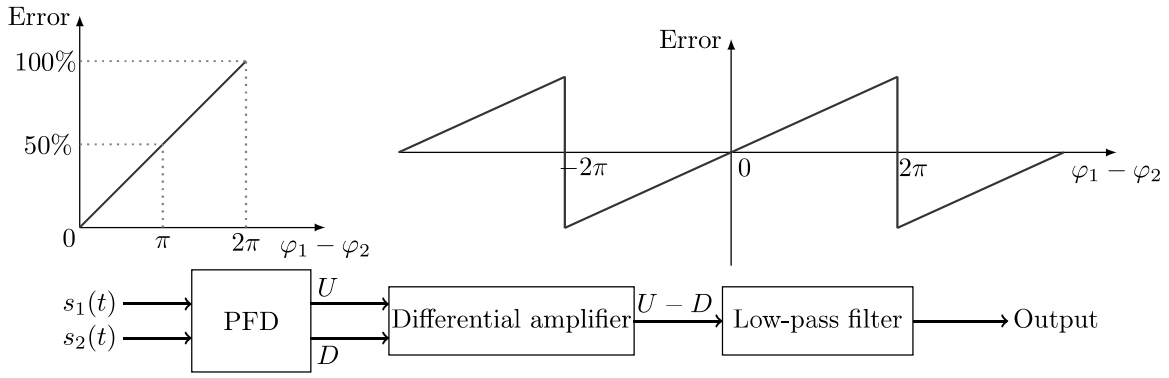

Figure 9: Left : Error signal created with a XOR gate. The unit of error signal is the percentage of the amplitude of the voltage of the square signal. Right : Output of the PFD set-up when $\omega_1 = \omega_2$.
Bottom : Schema of the PFD set-up

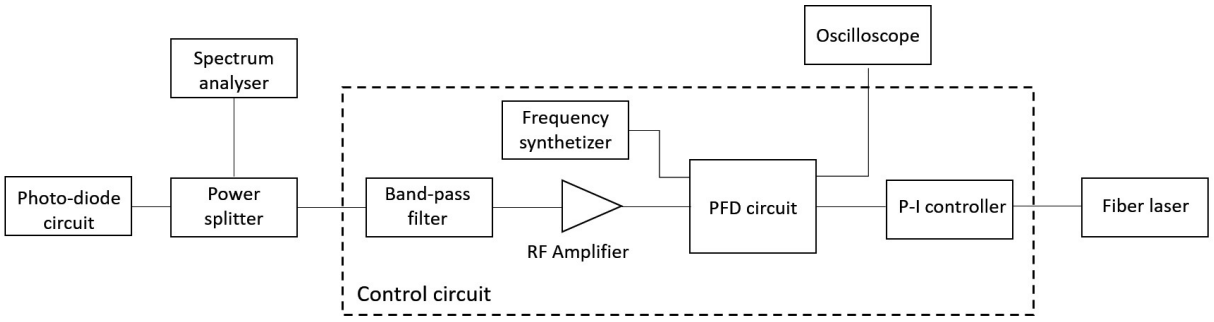

Figure 10: Overall schema of the control circuit. Power splitter[5]: MiniCircuits ZX10-2-12-5. Tunable band-pass filter : Telonic Berkeley TTF 250-5-5EE. Oscilloscope : Tektronix TDS 1012. Amplifier : MiniCircuits ZFL-500+

4 Results

In order to characterize our control, we made two kinds of acquisitions : we measured the frequency of the fiber laser with and without control, and also the phase noise, which is the signal in output of the PFD set-up.

4.1 Frequency measurement

We measured the frequency of the fiber laser with a commercial High Finesse WS7 wavemeter to know to what extent it was fluctuating. The idea was to compare the measured laser frequency under locked and non-locked conditions. In order to characterize the stability, we used the Allan deviation, which is computed in Figure 12 with `adev` function from the `allantools` library of *Python*.
Given a time-series $x(t)$ of the measurement of an oscillator, the Allan variance permits to measure its stability and it is defined as :

$$\sigma_y^2(\tau) = \left\langle (\bar{y}_{n+1} - \bar{y}_n)^2 \right\rangle \tag{4.1}$$

with $\bar{y}_n$ defined as :

$$\bar{y}_n = \frac{x\,(n\tau + \tau) - x(n\tau)}{\tau} \tag{4.2}$$

It means that the time-series is cut in two, then the means of the two parts are computed and we look at the variance of these two means. Next it is cut in four, and so on. Therefore, it is interesting to have a number of points that is a power of two.
Finally, the Allan deviation (which is computed by `adev`) is given by :

$$\sigma_y(\tau) = \sqrt{\sigma_y^2(\tau)} \tag{4.3}$$

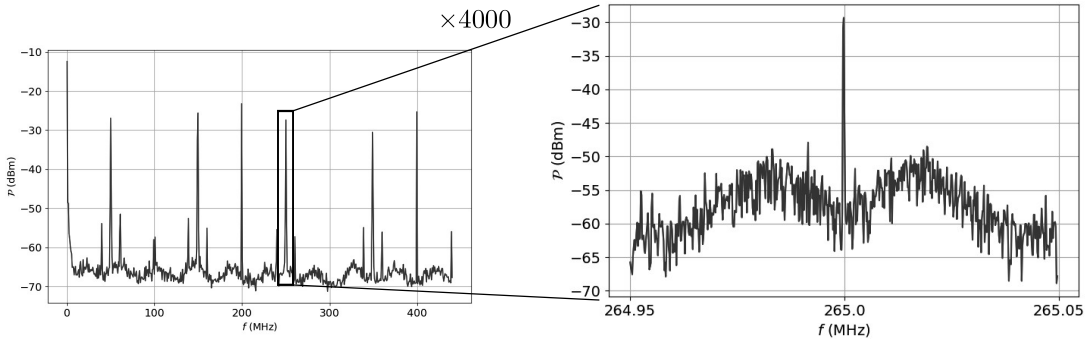

Figure 11: Beat-note under locked condition. Bandwidth : 100 Hz. Span : 100 kHz (Zoom : ×4000)

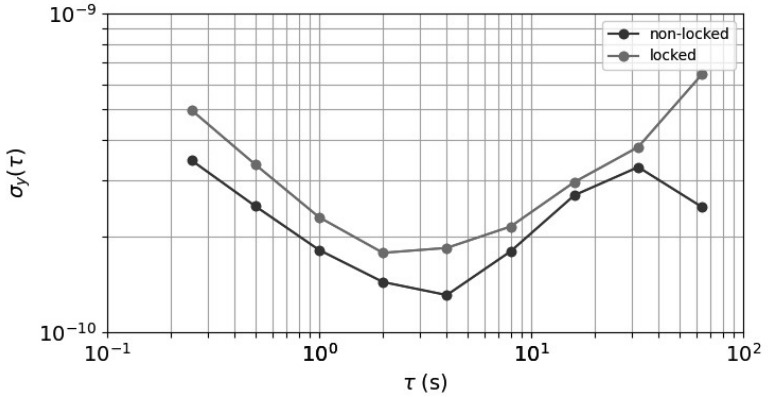

Figure 12: Allan deviations of the frequency of the fiber laser under locked and non-locked conditions

It could appear that the laser is more stable when unlocked, which is surprising. In fact, the wavemeter's resolution (ability to distinguish two different frequencies) is better than 2 MHz according to the documentation. Nevertheless, the Allan deviation on a frequency of approximately 285 THz is under 10^{-9} here, so the fluctuations are under 285 kHz in all the measured time scales. It is under the precision of the wavemeter, so it appears in fact that we have measured the fluctuations of the device and not of the laser. Even when it is unlocked, the fiber laser is more stable than the wavemeter.
In fact, the average laser frequency is controlled to better than 1 Hz. This measurement was made by a frequency counter with a very stable reference from the SYRTE laboratory. It is more than we need for the Doppler cooling (we need an accuracy better than 100 kHz).

4.2 Phase noise

At the output of the PFD set-up, there is a voltage error signal. When the frequency synthetizer emits at a frequency near the beat-note's one, we can see triangles on the oscilloscope, like in Figure 9. When we put the controller in place, the signal fluctuates near zero. But there is always a phase noise, that we are going to characterize.
Firstly, with the measurement of the amplitude of the error signal and its periodicity, we obtained the slope of the triangle signal and then we could access the phase error in radians. Then, thanks to the Wiener-Khintchine's theorem, we obtained the phase spectral density of the signal :

$$S_\phi(f) = |\Phi(f)|^2 \tag{4.4}$$

where $\Phi(f)$ is the Fourier transform of $\phi(t)$ the phase error. In general, we use rather the frequency spectral density of the signal, which is given by :

$$S_{\delta\nu}(f) = f^2 S_\phi(f) \tag{4.5}$$

In pratice, with the software *LabView* and a data acquisition board NI 6024, we measured the signal and computed the frequency spectral density. *LabView* gives a result in V^2, that we could call $S_U(f)\delta f$, with δf the frequency sampling step. We could transform it in $S_\phi(f)$ with the slope of the PFD, in

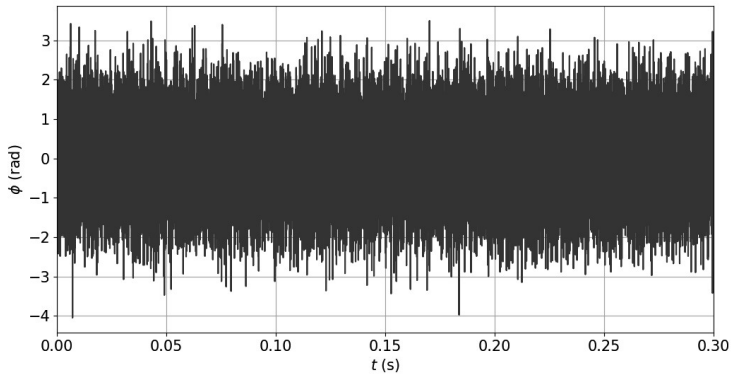

Figure 13: Error signal when the control is optimized. Number of samples : 60000. Sampling rate : 100000 Hz

order to obtain a result in rad^2/Hz. The triangular error signal's root mean square (RMS) amplitude is $U_{RMS} = 6,918$ V, and its period is 32π, because there is a 8-times-divider in the input of the PFD circuit, so the slope is $2U_{RMS}\sqrt{2}/32\pi \simeq 1.9.10^{-1}$ V.rad^{-1}. With this data, we could access the phase noise's standard deviation, which was approximately $0,943$ rad when the laser was well locked as in section 3.3.2. The computation was made with *Python* and `numpy.std()` function.
Then, we compared the frequency spectral density of noise when the laser was well locked and when the controller was badly settled. For this comparison, we put the coefficient for the integrator term at the minimum and the one for the proportional term very low.

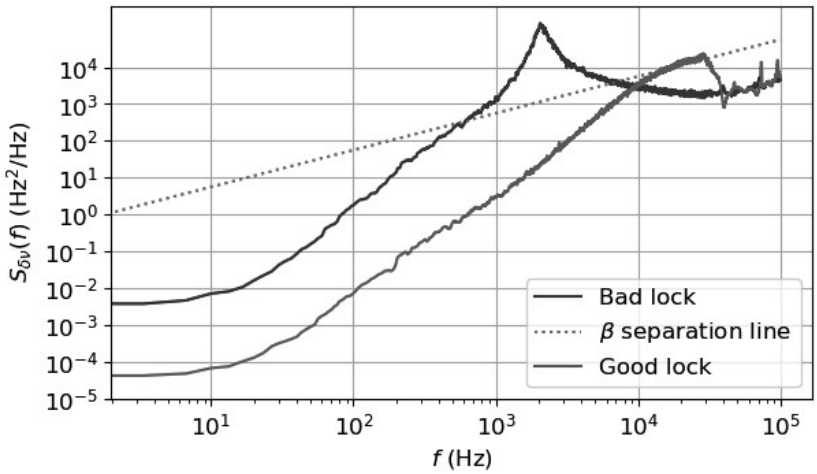

Figure 14: Frequency spectral densities of noise comparison

On Figure 14, we also traced the "β-separation line", whose equation is given by :

$$y = \frac{8\ln(2)f}{\pi^2} \tag{4.6}$$

It has been introduced by Di Domenico and al. [15]. This line separates the spectrum into two areas that contributes differently to the noise. To the right of the line, the contribution is for the wings of the beat-note and not for the laser lineditwh, whereas to the left, the contribution is for the laser linewidth. In [15], it is applied for a "low-pass filtered white noise", which means that a cutoff frequency f_c exists and :

$$S_{\delta\nu}(f) = \begin{cases} h_0 & \text{if } f \leq f_c \\ 0 & \text{if } f > f_c \end{cases} \tag{4.7}$$

Actually, Di Domenico and al. show that the only condition that is needed to apply the results is :

$$\forall (f_1, f_2),\ S_{\delta\nu}(f_1) \text{ and } S_{\delta\nu}(f_2) \text{ are independent random variables} \tag{4.8}$$

We will formulate this hypothesis for the rest of the paper.

5 Discussion

5.1 Conclusions on the control

Our wavemeter's precision is to low to compare the fluctuations of the locked and unlocked fiber laser, so we can think about more precise ways to do it. A solution could be to use another wavemeter, like the HighFinesse WS8-10 or WS8-2, that have better resolutions than 400 and 200 kHz. But in fact, we know that the average frequency is enough controlled for the Doppler cooling (we wanted an accuracy below 100 kHz$\simeq \Gamma/200$ and we got one which is below 1 Hz).
Moreover, Figure 14 shows that when the laser is well controlled, the frequency spectral density of noise is almost always underneath the β-separation line, so we can think that the noise contributes to the wings and little to the linewidth. However, when we put the integrator and proportional terms very low, the frequency spectral density of noise cross the β-separation line, and the linewidth is noisy. It appears that the linewidth is thin only if the laser is well locked.
To be more complete on our analysis, we could compare with the density of noise when the laser is unlocked. Nevertheless, there is a problem, which is that if the phase exceeds 32π, the PFD set-up take it back to zero. It is needed to implement a code that recognize the brutal changes in order to rebuild the phase signal.

5.2 Possibility of improvement

The bandwidth of feedback can be improved. Currently, the control loop affects the piezoelectric ceramic of the fiber laser and it is quite slow. But an electro-optic modulator (EOM) can be added in the circuit, allowing for bandwidth of tens of MHz. It is based on the electro-optic effect, which is the dependance of the index of refraction to a voltage applied accross a cristal. It is used to electrically control the phase shift undergone by a laser beam crossing the crystal.

6 Conclusion

The need of Be^+ ions Doppler cooling has led us to review the Doppler cooling theory, as well as some principles of nonlinear optics. Once the purpose was clarified, we demonstrated the implementation of a fiber laser control circuit. In order to lock the fiber laser on the frequency comb, we obtained the beat-note between these sources. We needed a PFD set-up in order to generate an error signal between the beat-note and a reference. Then, we put this signal to zero with a PI controller. There was always a frequency noise, and we characterized it with the β-separation line, introduced by Di Domenico and al. The main conclusion is that when the laser is well locked, the noise contributes to the wings of the lined shape and little to the linewidth, so it is possible to obtain a very thin linewidth of the fiber laser. Now, we can use this controlled laser for the Doppler cooling of Be^+. We can think that the cooling will be more efficient, because if the laser spectrum is thiner, there are less not interesting frequencies, that in some cases warm the ions instead of cooling them (there is a resonance that must not be exceeded).

References

1. Mohr, P. J., Newell, D. B. & Taylor, B. N. CODATA Recommended Values of the Fundamental Physical Constants: 2014. *Reviews of Modern Physics* **88,** 035009. ISSN: 0034-6861, 1539-0756. arXiv: 1507.07956 [physics]. (2024) (Sept. 2016).
2. Sturm, S. *et al.* High-Precision Measurement of the Atomic Mass of the Electron. *Nature* **506,** 467–470. ISSN: 0028-0836, 1476-4687. arXiv: 1406.5590 [physics]. (2024) (Feb. 2014).
3. Heiße, F. *et al.* High-Precision Measurement of the Proton's Atomic Mass. *Physical Review Letters* **119,** 033001. ISSN: 0031-9007, 1079-7114. arXiv: 1706.06780 [physics]. (2024) (July 2017).
4. Wing, W. H., Ruff, G. A., Lamb, W. E. & Spezeski, J. J. Observation of the Infrared Spectrum of the Hydrogen Molecular Ion H${\mathrm{D}}^{+}$. *Physical Review Letters* **36,** 1488–1491. (2024) (June 1976).
5. Hilico, L. Polarisabilities, Light Shifts and Two-photon Transition Probabilities between J=0 States of the H2 and D2 Molecular Ions. *Journal of Physics B-Atomic Molecular and Optical Physics* **34.** ISSN: 0953-4075 (Jan. 2001).
6. Karr, J.-P., Hilico, L., Koelemeij, J. C. J. & Korobov, V. Hydrogen Molecular Ions for Improved Determination of Fundamental Constants. *Physical Review A* **94,** 050501. (2024) (Nov. 2016).
7. Louvradoux, T. *Spectroscopie à haute résolution de H2+ : production et refroidissement sympathique d'ions piégés.* PhD thesis (Université Paris Cité, Dec. 2019). (2023).
8. Wineland, D. J., Drullinger, R. E. & Walls, F. L. Radiation-Pressure Cooling of Bound Resonant Absorbers. *Physical Review Letters* **40,** 1639–1642. (2024) (June 1978).
9. Drullinger, R. E., Wineland, D. J. & Bergquist, J. C. High-Resolution Optical Spectra of Laser Cooled Ions. *Applied physics* **22,** 365–368. ISSN: 1432-0630. (2024) (Aug. 1980).
10. Paul, W., Reinhard, H. P. & von Zahn, U. Das elektrische Massenfilter als Massenspektrometer und Isotopentrenner. *Zeitschrift für Physik* **152,** 143–182. ISSN: 0044-3328. (2024) (Apr. 1958).
11. Hänsch, T. W. & Schawlow, A. L. Cooling of Gases by Laser Radiation. *Optics Communications* **13,** 68–69. ISSN: 0030-4018. (2024) (Jan. 1975).
12. Wilson, A. C. *et al.* A 750 mW, Continuous-Wave, Solid-State Laser Source at 313 Nm for Cooling and Manipulating Trapped 9Be+ Ions. *Applied Physics B* **105,** 741–748. ISSN: 0946-2171, 1432-0649. arXiv: 1105.5356 [physics, physics:quant-ph]. (2024) (Dec. 2011).
13. Heinrich, J. *A Be+ Ion Trap for H2+ Spectroscopy* PhD thesis (Sorbonne Université, Apr. 2018). (2023).
14. Boyd, R. W. & Prato, D. *Nonlinear Optics* ISBN: 978-0-08-048596-6. (2024) (Elsevier Science & Technology, San Diego, UNITED STATES, 2008).
15. Di Domenico, G., Schilt, S. & Thomann, P. Simple Approach to the Relation between Laser Frequency Noise and Laser Line Shape. *Applied Optics* **49,** 4801–4807. ISSN: 1539-4522 (Sept. 2010).